Eur. Phys. J. Spec. Top.
https://doi.org/10.1140/epjs/s11734-026-02270-6

THE EUROPEAN PHYSICAL JOURNAL SPECIAL TOPICS

Regular Article

Partial decomposition of information dynamics elicits unique and shared modes of cardiovascular and cardiorespiratory control in response to autonomic stressors

R. Saputo[1,a], C. Barà[1,2], I. Franzone[1], M. Javorka[3], R. Pernice[1], and L. Faes[1,4,b]

[1] Department of Engineering, University of Palermo, Palermo, Italy
[2] Institute of Intelligent Industrial Technologies and Systems for Advanced Manufacturing, National Research Council, Milan, Italy
[3] Department of Physiology, Comenius University in Bratislava, Jessenius Faculty, Martin, Slovakia
[4] Faculty of Technical Sciences, University of Novi Sad, Novi Sad, Serbia

Received 30 November 2025 / Accepted 13 March 2026

Abstract The analysis of complex physiological systems increasingly relies on multivariate approaches that capture the dynamic interactions within and between interdependent subsystems. One promising measure in this context is the predictive information (PI), quantifying the amounts of Shannon information that is dynamically shared among past and future states of a multivariate system. While the PI is often decomposed using standard information theory, in this work we demonstrate that the emerging tool of partial information decomposition (PID) allows a better separation of unique and shared (redundant or synergistic) contributions of the past dynamics of the two components of a bivariate system to the present state of a designated target system. The proposed decomposition is applied to the study of the short-term regulation of heart period (HP) variability assessed in conjunction with systolic arterial pressure (SAP) variability to describe cardiovascular (CV) dynamics, or with respiration (RESP) variability to describe cardiorespiratory (CR) dynamics. The framework is implemented using both model-free and model-based estimators and applied to HP, SAP and RESP time series measured in young healthy subjects at rest state and during postural or mental stress. We observe that HP predictive dynamics are strongly determined by unique self-influences, which play a major role in driving the changes in process regularity observed moving from rest to postural and mental stress, and that the variations across conditions of the measures of CV and CR coupling are determined predominantly by the atoms of shared information (redundant and/or synergistic). Overall, our findings highlight the relevance of decomposing the PI by means of the PID tools for assessing information dynamics in physiological networks and their potential for identifying novel markers of autonomic control.

1 Introduction

The study of the dynamics of complex systems has become a central paradigm in contemporary science, as many natural processes emerge from the interaction of multiple, interdependent components [1]. In physiology, the human body can be described as a network of interconnected systems, where cardiovascular, respiratory, neural, and other subsystems continuously exchange information [2]. This networked organization, commonly referred to as "network physiology", highlights the importance of analyzing not only the behavior of individual systems, but also the patterns of interaction that sustain integrated regulation and adaptation [2, 3]. Within this framework, the cardiovascular (CV) and cardiorespiratory (CR) control systems represent two key network nodes whose dynamic interactions provide fundamental insights into autonomic regulation [4–6]. These interactions involve several important physiological mechanisms, including the arterial baroreflex as a basic reflex mechanism connecting

[a] e-mail: roberta.saputo@unipa.it
[b] e-mail: luca.faes@unipa.it (corresponding author)

Published online: 15 April 2026

blood pressure oscillations with heart rate response and the respiratory sinus arrhythmia (RSA) characterized by an effect of respiration on heart rate. The arterial baroreflex, by involving blood pressure and heart rate control, provides beat-to-beat negative feedback regulation of arterial blood pressure that minimizes short-term fluctuations in pressure [6]. The RSA is the physiological phenomenon whereby heart rate increases during inspiration and decreases during expiration and represents the strongest CR coupling, accounting for 20–60% of short-term heart rate variability at rest [4]. There is a large literature showing that physiological or psychological stress influences CV and CR regulation, altering their interactions [7–12]. The autonomic nervous system plays a central role in mediating CV and CR adjustments in response to physiological stressors. The transition to the upright position induces a rapid shift in autonomic balance, characterized by sympathetic activation and parasympathetic withdrawal, which supports blood pressure stabilization and heart rate acceleration, and is typically associated with an increased respiratory rate and a reduced respiratory-driven vagal modulation [13].

The above-mentioned physiological mechanisms can be studied effectively through the analysis of bivariate interactions between physiological time series of heart period (HP) and systolic arterial pressure (SAP)[14, 15], as well as between HP and respiration (RESP) amplitude [16, 17]. Besides traditional techniques, a comprehensive approach to perform such a description is framed in the field of information dynamics [18]. A measure of great interest in this context is the so-called predictive information (PI), quantifying the total amount of Shannon information that flows over time from the past to the present state of a multivariate process [19, 20]. In the bivariate setting, the PI measured between the present state of an individual "target" system and the past states of the whole bivariate system has been decomposed, exploiting Shannon information theory and the properties of mutual information (MI), to localize the contributions related to internal dynamics in the target system and those related to dynamic interactions originating in the other "driver" systems and directed to the target [21–23]. The resulting PI decompositions constitute a crucial development in information dynamics as they evidence core quantities related to the information contained in the target system, like the self entropy (SE) [24] or its conditional version (cSE) [22], or transferred to it from the driver system, like the transfer entropy (TE) [25] or the cross-entropy (CE) [22]. In computational physiology, the separate analysis of these quantities allowed to gain insights on the mechanisms related to autonomic control of HP, independently and in relation to SAP or RESP, as done in several works [8, 26–28], including important contributions from Danuta Makowiec [29–32].

In spite of their acknowledged potential, the measures derived from the decomposition of the PI of bivariate systems may fail to fully distinguish dynamic statistical relations due to directed interactions between the systems from internal relations occurring within an individual system. This issue has been raised regarding the SE as a measure of information storage within a system, as it was shown that it can reflect not only self-predictability but also causal effects [21], and also regarding the TE as a measure of directed information transfer between systems, as it was shown that it can contain information about the target that is not only coming from the driver but is also co-localized with the target itself [33]. The same critiques hold for CE and cSE measures which can be defined via a different decomposition of the PI [22]. To tackle this problem, the aim of the present study is to adopt a more stratified decomposition strategy which allows to isolate, within the measures derived from the PI, the contributions exclusively due to one system from those shared with the other system. To do this, we adopt the framework of partial information decomposition (PID), which constitutes a comprehensive tool to dissect information in multivariate systems [34, 35]. PID has been conceived in the framework of random variables to decompose the information that a "target" variable shares with a set of "source" variables into components highlighting how such an information is distributed among the sources, i.e., how this is uniquely related to a specific source or how it raises from the information redundantly and synergistically shared by the whole sources. Here, the framework is applied in the context of random processes, taking the present state of the analyzed target process as the target variable, and the past states of the target and driver processes (analyzed collectively) as source variables. In this way, the application of PID corresponds to decompose the PI into unique atoms of information, carrying information exclusively attributed to one system, and redundant and synergistic atoms, carrying information shared between the two systems.

In this work, the proposed approach applying the PID decomposition to the PI of bivariate dynamic systems is implemented in the practical analysis of bivariate time series taken from the CV system (HP and SAP) and from the CR system (HP and RESP) measured in a group of young healthy subjects monitored at rest and during both postural and cognitive load. The goal of the analysis was to investigate the improvement brought to the assessment of physiological mechanisms of CV and CR regulation by dissecting the traditional SE, TE, CE and cSE measures into quantities evidencing unique and shared contributions of the two dynamic systems analyzed. The effect of using different PID strategies based on distinct redundancy definitions (i.e., specific MI [34] and minimum MI [36]) and estimation approaches (respectively, nonlinear model-free for discrete random variables and linear model-based for continuous Gaussian random variables) is also investigated.

2 Methods

2.1 Predictive information decomposition

Given a bivariate dynamic system $\mathcal{S}$ composed of two possibly interacting subsystems $\mathcal{X}$ and $\mathcal{Y}$ whose dynamic evolution is represented by the process $S = \{X, Y\}$, let us denote as X_n and Y_n the states of the driver process X and the target process Y considered at the current time n, as $X_n^m = [X_{n-1}, \ldots, X_{n-m}]$ and $Y_n^m = [Y_{n-1}, \ldots, Y_{n-m}]$ the joint states of the two processes covered until m lags in the past, and as $X_n^- = \lim_{m\to\infty} X_n^m$ and $Y_n^- = \lim_{m\to\infty} Y_n^m$ their whole past history. The PI measures the part of the information carried by the present of the target, Y_n, that can be predicted by the past of the entire joint process, $[X_n^-, Y_n^-]$, and is quantified as [22]:

$$P_Y = I(Y_n; X_n^-, Y_n^-) = H(Y_n) - H(Y_n|X_n^-, Y_n^-), \tag{1}$$

where $I(\cdot;\cdot)$ denotes mutual information (MI), $H(\cdot)$ denotes entropy and $H(\cdot|\cdot)$ denotes conditional entropy.

In an attempt to separate the statistical dependencies arising from each of the two systems, the PI can be decomposed exploiting the chain rule for MI and expressed as the sum of two contributions of information dynamics as follows [22]:

$$P_Y = S_Y + T_{X\to Y}, \tag{2}$$

$$P_Y = C_{X\to Y} + S_{X|Y}. \tag{3}$$

The two alternative decompositions (2) and (3) evidence two quantities which have been related to the individual dynamics of the target process Y, i.e., S_Y and $S_{Y|X}$, and two other quantities which have been related to the directed interactions from the driver to the target process, i.e., $T_{X\to Y}$ and $C_{X\to Y}$. In particular, the SE, defined as

$$S_Y = I(Y_n; Y_n^-), \tag{4}$$

quantifies the part of the information carried by the present of the target process that can be predicted by its own past, and is associated to the regularity of the process [24], while the cSE, defined as

$$S_{Y|X} = I(Y_n; Y_n^-|X_n^-) = I(Y_n; Y_n^-, X_n^-) - I(Y_n; X_n^-), \tag{5}$$

quantifies the part of the information carried by the present of the target process that can be predicted by its past above and beyond the part that was predicted by the past of the driver, and is associated to the internal dynamics of the target [22]. On the other hand, the CE, defined as

$$C_{X\to Y} = I(Y_n; X_n^-), \tag{6}$$

quantifies the part of the information carried by the present of the target that can be predicted by the past of the driver, and is associated to the cross-predictability of target given the driver history [37], while the TE, defined as

$$T_{X\to Y} = I(Y_n; X_n^-|Y_n^-) = I(Y_n; Y_n^-, X_n^-) - I(Y_n; Y_n^-), \tag{7}$$

quantifies the part of the information carried by the present of the target process that can be predicted by the past of the driver and that cannot be already predicted by the past of the target, and is associated to the causal information transfer from driver to target [25].

2.2 Partial information decomposition

Let us consider three possibly correlated random variables, of which one is denoted as target variable, T, and the remaining two as source variables, S_1 and S_2. The framework of Partial Information Decomposition (PID) introduced in the seminal work of Williams and Beer [34] allows to decompose the information shared by the target with the two sources, quantified by the MI $I(T; S_1, S_2)$ and the redundancy term, in four distinct and non-negative quantities:

$$I(T; S_1, S_2) = \mathcal{U}(T; S_1) + \mathcal{U}(T; S_2) + \mathcal{R}(T; S_1, S_2) + \mathcal{S}(T; S_1, S_2), \tag{8}$$

where $\mathcal{U}(T;S_1)$ and $\mathcal{U}(T;S_2)$ are the information contributions exclusively provided to the target by one of the two sources, $\mathcal{R}(T;S_1,\,S_2)$ is the information about the target held redundantly by both sources, and $\mathcal{S}(T;S_1,\,S_2)$ is the synergistic information that only arises when both the sources are known and that cannot be inferred when considering any of them separately.

Exploiting the rules underlying the structure of the so-called redundancy lattice shown in Fig. 1a, the terms of this decomposition can be expressed using Shannon MI quantities as follows [34]:

$$\mathcal{U}(T;S_1) = I(T;S_1) - \mathcal{R}(T;S_1,\,S_2), \tag{9}$$

$$\mathcal{U}(T;S_2) = I(T;S_2) - \mathcal{R}(T;S_1,\,S_2), \tag{10}$$

$$\mathcal{S}(T;S_1,\,S_2) = I(T;S_1,\,S_2) - \mathcal{U}(T;S_1) - \mathcal{U}(T;S_2) - \mathcal{R}(T;S_1,\,S_2). \tag{11}$$

Since the consistency equations in Eqs. (9–11) identify a system of three equations and four unknown variables, to solve the PID problem it is necessary to introduce a fourth equation defining the redundancy measure $\mathcal{R}(T;S_1,\,S_2)$. This is an open issue in information theory, with several definitions proposed satisfying a set of partially different requirements about the properties that a redundancy measure should satisfy [35]. Two of the possible choices are presented in Sect. 2.4, and implemented with the target and source variables presented in Sect. 2.3.

2.3 Partial information decomposition of predictive information

This section presents the original contribution of the present work, which is to show how the terms appearing in the decomposition of the PI can be represented by combining PID atoms, and therefore can be dissected to evidence separate unique and shared contributions. The idea underlying our approach is to embed PID into the decomposition of the PI, so as to refine such decomposition making it more fine-grained. To this end, we consider that the quantity we start from, i.e. the PI defined in (1), is a mutual information between a scalar variable and a pair of other (vector) variables and, as such, it can be decomposed usig the PID defined in (8).

Specifically, we assume the present of the target process as the target variable for the PID, i.e., $T = Y_n$, and the past of the target and driver processes as the two sources, i.e., $S_1 = Y_n^-$ and $S_2 = X_n^-$, and then we apply the PID defined in Sect. 2.2 to the PI defined in Sect. 2.1. Combining Eqs. (4) and (9), as well as combining Eqs. (6) and (10), it is straightforward to see that the SE, S_Y, and the CE, $C_{X\to Y}$, can be decomposed as

$$S_Y = \mathcal{U}(Y_n;Y_n^-) + \mathcal{R}(Y_n;Y_n^-,\,X_n^-), \tag{12}$$

$$C_{X\to Y} = \mathcal{U}(Y_n;X_n^-) + \mathcal{R}(Y_n;Y_n^-,\,X_n^-), \tag{13}$$

showing how the information stored in the target process Y results from the unique contribution to Y_n provided exclusively by Y_n^- plus the shared contribution provided redundantly by both Y_n^- and X_n^-, and how the cross-information between the past of the driver process X and the present of the target process Y results from the unique contribution to Y_n provided exclusively by X_n^- plus a shared contribution provided redundantly by both Y_n^- and X_n^-.

On the other hand, combining Eqs. (7) and (9, 11), and combining Eqs. (5) and (10, 11), one can see that the TE, $T_{X\to Y}$, and the cSE, $S_{Y|X}$, can be decomposed as

$$T_{X\to Y} = \mathcal{U}(Y_n;X_n^-) + \mathcal{S}(Y_n;Y_n^-,\,X_n^-), \tag{14}$$

$$S_{Y|X} = \mathcal{U}(Y_n;Y_n^-) + \mathcal{S}(Y_n;Y_n^-,\,X_n^-), \tag{15}$$

showing how the information transferred from the driver process X to the target process Y results from the unique contribution to Y_n provided exclusively by X_n^- plus the shared contribution provided synergistically by both Y_n^- and X_n^-, and how the internal information in the target process Y not arising from the driver process X and results from the unique contribution to Y_n provided exclusively by Y_n^- plus the shared contribution provided synergistically by both Y_n^- and X_n^-.

The two decompositions highlighted by Eqs. (12, 13) and by Eqs. (14, 15) are illustrated exploiting the PID lattice structure in Fig. 1b, c.

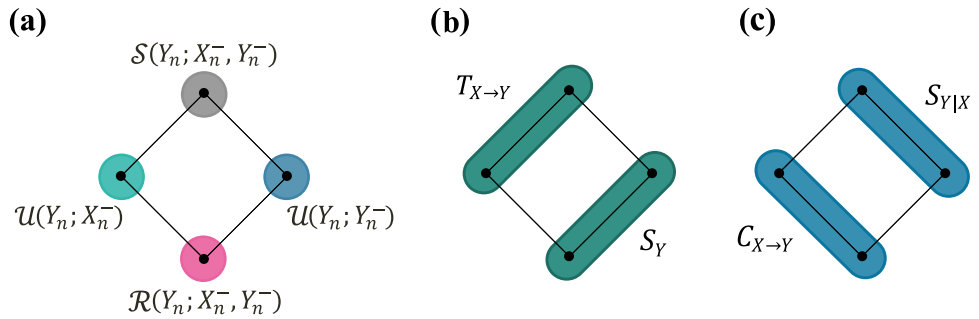

Fig. 1 In panel (**a**), the redundancy lattice representing the PID atoms used to decompose the Predictive Information measure P_Y is depicted, i.e., the unique contributions $\mathcal{U}(Y_n; X_n^-)$ and $\mathcal{U}(Y_n; Y_n^-)$, as well as the redundant and the synergistic contributions $\mathcal{R}(Y_n; Y_n^-, X_n^-)$ and $\mathcal{S}(Y_n; Y_n^-, X_n^-)$. Panels (**b**) and (**c**) depict how the PID atoms are aggregated to yield the decomposition terms in Eqs. (2) and (3)

2.4 PID estimation strategies

In order to implement the framework for the analysis of bivariate dynamic systems described in Sect. 2, it is necessary (i) to solve the PID problem by defining an appropriate redundancy measure, and (ii) to develop estimators of such redundancy measure, as well as of the remaining three PID quantities (Eqs. (9–11)), which, combined as in Eqs. (12–15), yield estimates of the SE, CE, TE, and cSE. As regards the first step, although there is no consensus in the literature about how to define the redundancy function unequivocally, several axiomatic definitions have been proposed so far that differ depending on the nature (continuous [36] or discrete [34]) of the variables representing the processes, and on the assumptions made about their distribution (e.g., Gaussian [36]). In this work, we exploited two different approaches based on model-free and model-based formulations, respectively, described in Sects. 2.4.1 and 2.4.2, to compute the redundancy function and solve the PID problem. These estimates can be carried out under the Markov assumption, approximating the past history of the processes up to m lags.

2.4.1 Model-free computation based on the specific mutual information PID

As proposed by Williams and Beer in their seminal work on PID [34], when working with discrete variables the information redundantly brought by the two source variables X_n^m and Y_n^m to the target variable Y_n can be defined as the minimum of information shared individually by the two source variables with a specific observation y_n of the target:

$$\mathcal{R}(Y_n; X_n^m, Y_n^m) = \sum_{y_n \in A_{Y_n}} p(Y_n = y_n) \min(I(Y_n = y_n; X_n^m),\, I(Y_n = y_n; Y_n^m)). \tag{16}$$

The specific MI quantities in Eq. (16) can be written as:

$$I(Y_n = y_n; X_n^m) = \sum_{x_n^m \in A_{X_n^m}} p(x_n^m|y_n) \log_2 \frac{p(x_n^m|y_n)}{p(x_n^m)}, \tag{17}$$

$$I(Y_n = y_n; Y_n^m) = \sum_{y_n^m \in A_{Y_n^m}} p(y_n^m|y_n) \log_2 \frac{p(y_n^m|y_n)}{p(y_n^m)}, \tag{18}$$

where $p(x_n^m)$ and $p(y_n^m)$ are the marginal probabilities of specific values of the variable X_n^m and Y_n^m belonging to the alphabet $A_{X_n^m}$ and $A_{Y_n^m}$, $p(x_n^m|y_n) = \frac{p(x_n^m, y_n)}{p(y_n)}$ and $p(y_n^m|y_n) = \frac{p(y_n^m, y_n)}{p(y_n)}$ are their probability conditioned on specific values of the target variable Y, with $p(y_n)$ being the marginal probability of the specific outcome $y_n \in A_{Y_n}$, and finally $p(x_n^m, y_n)$ and $p(y_n^m, y_n)$ represent its joint probability with x_n^m and y_n^m, respectively. Once the redundancy is determined as described in Eq. (16), the individual and joint MI terms needed to complete the PID as described in Eqs. (9–11) can be obtained as follows:

$$I(Y_n; X_n^m) = \sum_{y_n^m \in A_{y_n}} p(y_n) I(Y_n = y_n; X_n^m), \tag{19}$$

$$I(Y_n; Y_n^m) = \sum_{y_n^m \in A_{y_n}} p(y_n) I(Y_n = y_n; Y_n^m), \tag{20}$$

$$I(Y_n; X_n^m, Y_n^m) = \sum_{(y_n, x_n^m, y_n^m) \in A_{y_n, X_n^m, Y_n^m}} p(y_n, x_n^m, y_n^m) \log_2 \frac{p(y_n | x_n^m, x_n^m)}{p(y_n)}, \tag{21}$$

where $p(y_n, x_n^m, y_n^m)$ is the joint probability of y_n, x_n^m and y_n^m belonging to the alphabet A_{y_n, X_n^m, Y_n^m}, and $p(y_n|x_n^m, y_n^m)$ is the conditioned probability of y_n^m and x_n^m on y_n. In this work, all the above probabilities were estimated through the frequentistic approach applied to observations of the discrete random variables sampling the present and past states of the two analyzed processes; discrete-valued amplitudes were obtained through uniform quantization.

2.4.2 Linear parametric computation based on the minimum mutual information PID

A popular and simple approach to compute redundancy function is the so-called Minimum MI (MMI) PID [36]. With this approach, the information shared redundantly by the two sources X_n^m and Y_n^m with the target variable Y_n is defined as the minimum of the information shared between the target and each individual source:

$$\mathcal{R}(Y_n; X_n^m, Y_n^m) = \min(I(Y_n; X_n^m), I(Y_n; Y_n^m)). \tag{22}$$

Remarkably, when working with continuous-valued variables following a normal distribution, the MMI PID encompasses many other definitions of redundancy [36]. In this case, exploiting the tight connection between information measures and linear regression that holds for zero-mean jointly Gaussian variables [38], the two MI terms needed to compute redundancy can be computed using two parametric "reduced" models relating the target variable Y_n with the source variables X_n^m (cross-regressive model) and Y_n^m (autoregressive model):

$$Y_n = X_n^m A_X + U_{1,n}, \tag{23}$$

$$Y_n = Y_n^m A_Y + U_{2,n}, \tag{24}$$

where Y_n is predicted using the m-dimensional vector coefficients A_X and A_Y weighing the regressor X_n^m and Y_n^m, respectively, and U_1 and U_2 are zero-mean white Gaussian noises representing the prediction error of the two models. Then, the variance of the target variable σ_Y^2 and that of the prediction errors $\sigma_{U_1}^2$ and $\sigma_{U_2}^2$ are used to compute the MI between the target variable Y_n and the two source variables X_n^m and Y_n^m, as follows [38]:

$$I(Y_n; X_n^m) = \frac{1}{2} \log\left(\frac{\sigma_Y^2}{\sigma_{U_1}^2}\right), \tag{25}$$

$$I(Y_n; Y_n^m) = \frac{1}{2} \log\left(\frac{\sigma_Y^2}{\sigma_{U_2}^2}\right). \tag{26}$$

The MI terms in Eqs. (25, 26) are exploited both to compute the redundancy according to Eq. (22) and to derive the unique terms of PID according to Eqs. (9, 10). Finally, to compute synergy according to Eq. (11), the MI between the present of the target process Y and the joint past history of the two processes $\{X, Y\}$ is computed, from the parameters of a "full" regression model defined as

$$Y_n = X_n^p B_X + Y_n^p B_Y + U_n, \tag{27}$$

according to the equation

$$I(Y_n; X_n^p, Y_n^p) = \frac{1}{2} \log\left(\frac{\sigma_Y^2}{\sigma_U^2}\right), \tag{28}$$

where σ_U^2 is the variance of the white Gaussian noise U; note that the lag used to explore the past of the two processes here is the model order p. In practical analysis, the full model defined in Eq. (27) is identified through the ordinary least square (OLS) approach [39], while the parameters of "restricted" models defined in Eqs. (23) and (24) are obtained directly from those of the full model through a procedure that solves the associated Yule-Walker equations and determines the coefficients A_X and A_Y up to an order $m >> p$. The full estimation procedure is detailed in the supplemental material of [40], and in [41].

3 Application to physiological data

In this section, we present a physiological application to real data of the framework of analysis described in Sect. 2, aimed to investigate the intertwined CV and CR dynamics involved in the physiological control mechanisms that act in response to postural stress and cognitive load.

3.1 Experimental protocol

The study involved a group of 127 healthy young volunteers (75 females; age: 18.6 ± 3.3 years), all normotensive and with body mass index within the normal range (BMI: 21.4 ± 2.2 kg/m^2), recruited from the local elementary schools, high schools and the universities of Martin, Slovakia. According to the ethical principles of the Declaration of Helsinki for research studies involving human subjects, all participants or their legal guardian for minors (i.e., age < 18 years) signed a written informed consent to join the experimental study, which was approved by the Ethics Committee of the Jessenius Faculty of Medicine, Comenius University, Martin, Slovakia. Before starting the procedures, subjects were instructed to abstain from using any substances that could affect the autonomic nervous system or CV activity. Subsequently, each participant was positioned on a motorized tilt table with the feet touching the footboard at the end of the table, and a restraining strap secured at the thigh level was used to provide additional support and safety prior to initiating the protocol. The experimental protocol consists of five conditions, fully detailed in [42], of which only three were taken into account in this study:

1. Resting supine position (REST): subjects were laid on the motorized table in a horizontal position for 15 min to stabilize the physiological parameters at the baseline levels;
2. Head-Up Tilt (HUT): the motorized table was tilted to a 45° upright position for 8 min to evoke mild orthostatic stress;
3. Mental Arithmetic (MA): a mental arithmetic test was administered to participants in a supine position for 6 min to induce cognitive load.

The arithmetic test was performed using WQuick software with WIN 5 PMT test (Psycho Soft Software, s.r.o., Brno, Czech Republic). During the test, participants were instructed to sum up three-digit numbers until a one-digit number was obtained, finally deciding whether it was even or odd. Responses were given by clicking the corresponding virtual push button projected onto the ceiling via a computer mouse. To further increase the perceived stress during cognitive load task, participants were disturbed by the rhythmic sound of a metronome and instructed to perform the MA task as quickly as possible. Further details on the experimental protocol can be found in [43, 44].

3.2 Signal acquisition and time series extraction

Electrocardigraphic signal (ECG, horizontal bipolar thoracic lead; CardioFax ECG-9620, NihonKohden, Japan), continuous finger arterial blood pressure via the photoplethysmographic volume-clamp method (Finometer Pro, FMS, Netherlands), and respiratory volume through respiratory inductive plethysmography (RespiTrace 200; NIMS) were simultaneouly and non-invasively recorded at a sampling frequency of 1 kHz. Qualitative diagnostic calibration of the respiratory signal was followed by quantitative calibration, where partecipants breathed into a 1,000-ml plastic bag. All signals were digitalized and transferred to a personal computer at a sampling rate of 1 kHz using PowerLab 8/35 (ADInstruments) device. Further details on the signal acquisition can be found in [45].

Starting from the recorded signals, beat-to-beat variability time series were extracted for each subject in the three experimental conditions (i.e., REST, HUT, MA) as schematized in Fig. 2. Specifically, the n-th heart period (HP_n) value was computed as the temporal distance between two consecutive R-wave peaks of the ECG signal, i.e., n-th and $(n+1)$-th peaks with n being the heart rate counter, using the Pan–Tompkins QRS detection algorithm. The n-th sample of the systolic arterial pressure (SAP_n) time series was defined as the maximum value within the corresponding HP, while the correspondent sample in the time series of the respiration values (RESP_n) was obtained by sampling the respiratory volume signal at the onset of each detected HP_n.

To exclude transient effects in physiological parameters and favor the stationarity of the time series, windows of 300 consecutive heartbeats were extracted for the three time series, starting 8 min after the beginning of the REST phase, 3 min after the beginning of the HUT phase, 2 min after the beginning of the MA phase. The selected 300-point windows were free of artifacts, including those related to calibration of the Finometer device (such calibration, which interrupts the measurements of the continuous blood pressure signal, was executed only in the last minute of the REST phase).

Each time series was corrected to remove outliers beyond three standard deviations from the mean. These outliers were replaced using two different interpolation algorithms, i.e., linear for isolated outliers and cubic spline for

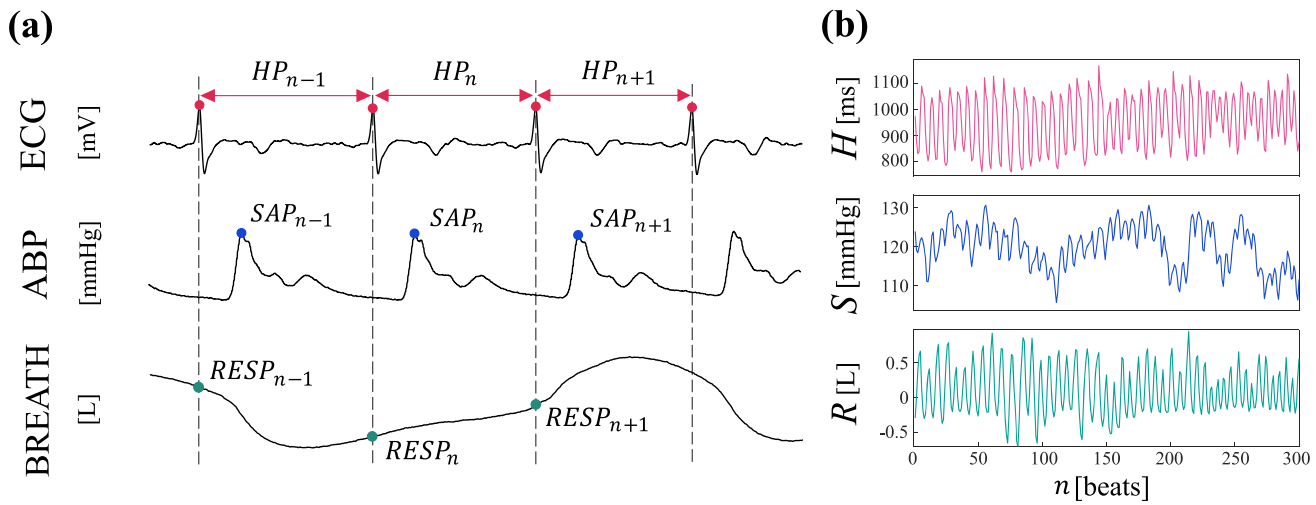

Fig. 2 **a** Schematic representation of the measurement of beat-to-beat variability time series of heart period (HP), systolic arterial pressure (SAP) and respiratory volume (RESP) from the recorded electrocadiographic (ECG), arterial blood pressure (ABP) and the respiratory volume (BREATH) signals; **b** example of H (top), S (middle) and R (bottom) time series for a representative subject in the REST condition

multiple successive ones. The corrected time series were visually inspected for any issues following the interpolation procedure. Overall, only 0.6% of the samples of each time series were adjusted, allowing a more reliable analysis. To remove the slow trends an auto-regressive high-pass filter (zero phase; cutoff frequency 0.0156 times the equivalent sampling rate of series) [46] was applied to the time series and the mean value was subsequently removed prior to the analysis to obtain zero-mean series.

In the following, the beat-to-beat variability time series of HP, SAP, and RESP will be labeled as H, S, and R, respectively.

3.3 Data analysis

Starting from the corrected H, S, and R time series, two separate analyses were conducted to compute PI and PID terms in CV and CR dynamics through both model-free and model-based formulations. For CV analysis, the bivariate system composed of the target process $Y = H$ and the driver process $X = S$ was considered, thus imposing the realizations of the current state of H (i.e., H_n) as target variable and those of the past states of H and S (i.e., H_n^- and S_n^-, respectively) as the two source variables of the PID. Specifically, the PI of H was calculated as the MI between H_n and S_n^- and H_n^-, i.e., $P_H = I(H_n; S_n^-, H_n^-)$, and then the PID was applied evidencing the unique contributions, denoted as $\mathcal{U}_H = \mathcal{U}(H_n; H_n^-)$ and $\mathcal{U}_S = \mathcal{U}(H_n; S_n^-)$, as well as the redundant and synergistic contributions, denoted as $\mathcal{R}_{H,S} = \mathcal{R}(H_n; H_n^-, S_n^-)$ and $\mathcal{S}_{H,S} = \mathcal{S}(H_n; H_n^-, S_n^-)$. Then, the SE, TE, cSE and CE measures were obtained as the sum of PID atoms as reported in Eqs. (12–15) and respectively denoted as S_H, $T_{S\to H}$, $S_{H|S}$ and $C_{S\to H}$. Similarly, for CR analysis, the bivariate system composed of the target process $Y = H$ and the driver process $X = R$ was considered. In this case, the PID terms $\mathcal{U}_H, \mathcal{U}_R, \mathcal{R}_{H,R}$ and $\mathcal{S}_{H,R}$, as well as the SE, TE, cSE and CE measures, denoted as S_H, $T_{R\to H}$, $S_{H|S}$, $C_{R\to H}$, were obtained decomposing the PI measure $P_H = I(H_n; R_n^-, H_n^-)$.

All measures were computed for each subject in the three experimental conditions (REST, HUT, MA) through both model-free and model-based formulations, resulting in information-theoretic measures expressed in bits and nats, respectively. Specifically, as regards the model-free analysis, the discretization method based on binning [47] was used to build discrete random variables through quantization of the continuous-valued variables, so as to estimate the probability distributions needed to compute the mutual information terms in Eqs. (17–21) via the frequentistic approach. The number of quantization levels and the length of the memory used to cover the past history of the processes were chosen equal to $b=6$ and $m=1$, respectively. These parameters were set in order to satisfy the empirical criterion $b^{2m+1} < N$ [47], with N the length of time series, which is used to limit the issue related to the estimation bias of information measures referred to high-dimensional variables from finite-size dataset (i.e., the so-called curse of dimensionality [48]).

On the other hand, as regards the model-based approach, the full linear parametric model defined in Eq. (27) and the reduced AR and X models in Eqs. (23) and (24) were separately fitted for CV and CR analyses, to compute the MI terms involved in the computation of the PID measures as described in Sect. 2.4.2. The order p of the full model was set according to the multivariate version of the Akaike Information Criterion (AIC) [49], with maximum

scanned model order equal to 12. The model order was estimated separately for each subject and experimental condition, obtaining mean values of $\mu_{AIC}^{CV} = [7; 7.5; 7.1]$ for CV analysis (respectively for REST, HUT and MA) and of $\mu_{AIC}^{CR} = [6.7; 7; 6.5]$) for CR analysis. The order m of the reduced models was fixed at 20, in accordance with previous works [40, 41].

3.4 Surrogate and statistical data analysis

To test the statistical significance of the aforementioned information measures in both CV and CR analysis, two different procedures for surrogate data generation were used for model-free and model-based formulations. As regards the model-free analysis, we followed the procedure described in [50] based on the shuffling of the target variable and aimed at assessing the statistical significance of each of the atoms of the redundancy lattice. In more detail, the significance of the information associated to each of the atoms of the lattice and for specific values of the target variable was assessed randomizing the order of the target samples and verifying that the value obtained on the original data is higher than the $(100 - \frac{0.05}{4b})$th percentile of the distribution obtained on surrogate data. As a consequence, the significance of all the PID terms, as well as of the PI decomposition quantities, was ascertained if at least one of the specific quantities forming it is significant. On the other hand, in the model-based approach the random shuffling of the order of the target samples was employed to obtain the surrogate data, and all measures were deemed as statistically significant if their values were above the 95th percentile of the surrogate distribution. The random shuffling surrogate approach was chosen since it destroys the autocorrelation between past and present values of the processes, which is necessary for more reliably assessing the significance of information-theoretic measures based on the dynamics of the signals [51]. One-hundred pairs of surrogate data were generated for each subject and condition by iterating both procedures in CV and CR analysis.

In order to assess statistically significant differences of the indices among different physiological conditions, parametric tests were used, since most distributions were normal according to Kolmogorov-Smirnov test ($\alpha = 0.05$) and given the large sample size. Specifically, one-way ANOVA test was performed to assess the statistical significance of the mean of the distribution among conditions (i.e., REST, HUT, MA) with a significance level of 5%. Then, a post-hoc Student t-test for paired data with Bonferroni correction for multiple comparisons ($n = 2$ comparisons, and thus $p = 0.05/2 = 0.025$) was employed to assess the statistical significance differences between pairs of distributions (i.e., HUT vs. REST, MA vs. REST). Finally, Student t-test was used to assess the statistically significant differences between redundancy and synergy in each condition, with a significance level of 5%.

4 Results

4.1 Predictive Information decomposition of cardiovascular dynamics

Figure 3 reports the results of the analysis of dynamic information measures performed through the model-free estimator for the assessment of CV interactions evaluated for each subject during REST, HUT and MA experimental conditions. All measures except $\mathcal{U}_S$ exhibit a statistically significant increase with the transition from the REST to the HUT phase. Moreover, P_H, S_H, $S_{H|S}$ and $\mathcal{U}_{\mathcal{H}}$ display also a statistically significant increase during MA compared to REST. The number of subjects (out of 127) exhibiting statistically significant values according to surrogate data analysis is high (i.e., greater than 103) for all measures evaluated with the model-free analysis, except for $\mathcal{U}_S$ (i.e., less than or equal to 12) and, even though with slightly higher values, for $T_{S\to H}$ and $\mathcal{S}_{H,S}$ (i.e., less than or equal to 55 and 50, respectively), as indicated by the number at the top of the corresponding measures. These results suggest that: (i) both postural and mental stress elicit an increased predictability of HP variability given its past and the past of SAP (Fig. 3a); (ii) using the traditional PI decomposition (Fig. 3b), the increase of PI is ascribed to an increase of the measures reflecting the self-dynamics of HP (i.e., SE and cSE) during both stressors and also to an increase of the measures reflecting coupled dynamics between HP and SAP (i.e., TE and CE) only during postural stress; (iii) using the PID decomposition of the PI (Fig. 3c), the increase of PI is ascribed to an increase of the unique of H, redundant and synergistic contributions during postural stress, but only of the unique contribution of HP during mental stress.

Figure 4 reports the results of the analysis of dynamic information measures performed through the model-based estimator for the assessment of CV interactions computed for each subject across the three experimental phases. All measures exhibit a statistically significant increase from REST to HUT, except for $\mathcal{U}_S$ which does not exhibit any significant change between REST and any stress condition (i.e., HUT vs. REST and MA vs. REST). $C_{S\to H}$ and $\mathcal{R}_{H,S}$ exhibit a statistically significant decrease, and $S_{H|S}$ and $\mathcal{U}_H$ a statistically significant increase, during MA compared to REST. Also for the model-based analysis, the number of subjects exhibiting statistically significant values is high for all measures except for $\mathcal{U}_S$. These results suggest that: (i) only postural stress elicits an increased predictability of HP variability given its past and the past of SAP (Fig. 4a); (ii) using the traditional

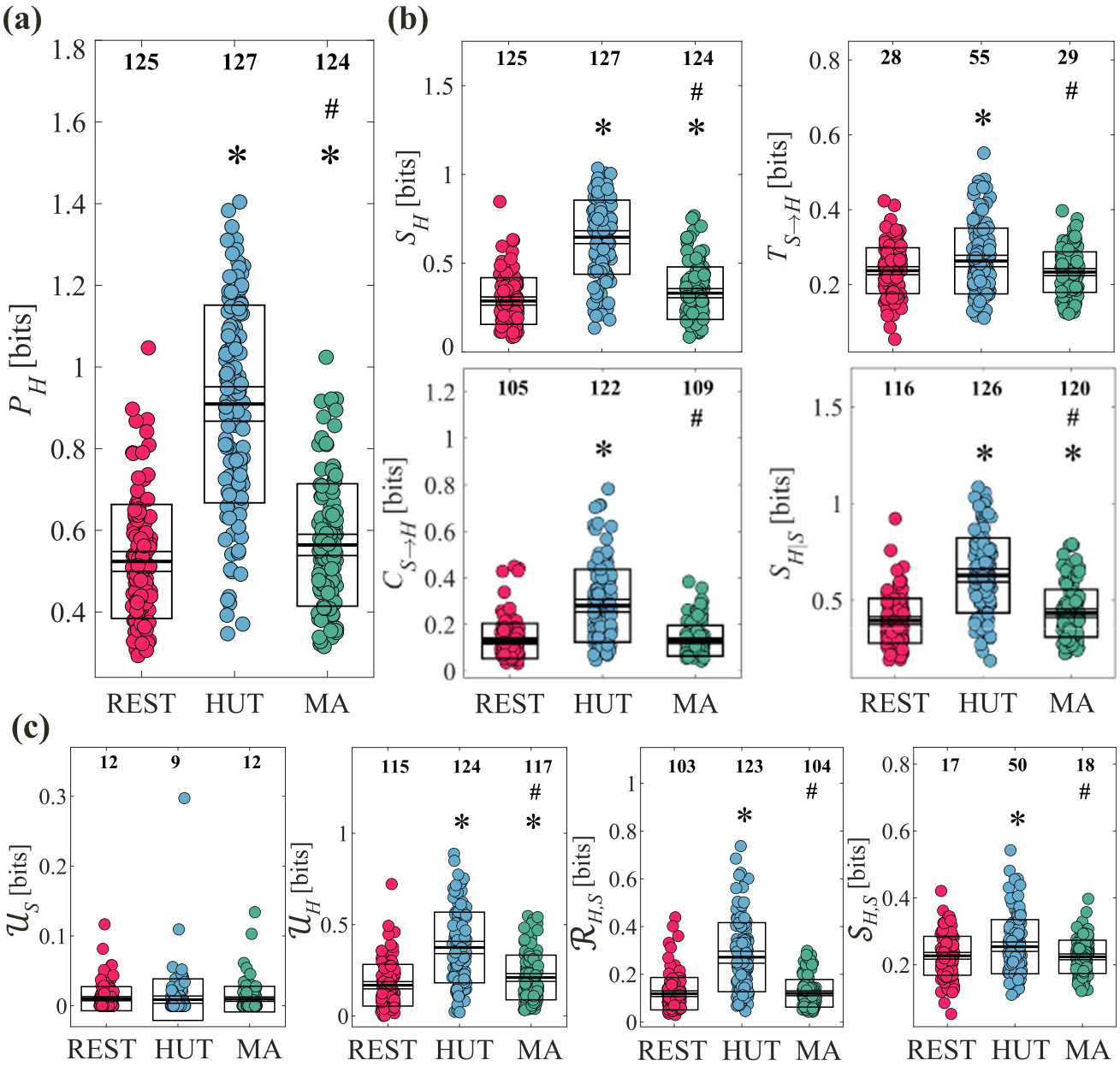

Fig. 3 Predictive Information decomposition of CV interactions obtained via model-free estimates of information dynamics. Plots depict the boxplot distributions and individual values (dots along the vertical lines) of **a** the Predictive Information of H (P_H), **b** the individual terms of the first and second decomposition of P_H given S, and **c** the unique, redundant and synergistic atoms of PID decomposing P_H given S. Measures were evaluated in the REST (red), HUT (blue), and MA (green) conditions. In all panels, black horizontal lines indicate mean values, while the white areas bounded by the box edges and by the lines surrounding the mean represent one standard deviation and the 95% confidence interval, respectively. One-way ANOVA test among conditions ($p < 0.05$): #. Student t-test for paired data with Bonferroni correction for multiple comparison ($p < 0.025$): *REST vs. HUT, REST vs. MA. Values above each distribution indicate the number of subjects (out of 127) for which the measure was deemed as statistically significant according to surrogate data analysis

PI decomposition (Fig. 4b), the increase of PI during postural stress involves all measures reflecting both self-dynamics and coupling, while the unchanged PI during mental stress results from a decreased cross-predictability together with an increased self-predictability of HP; (iii) using the PID decomposition of the PI (Fig. 4c), the increase of PI during postural stress is due to an increase of the unique contribution of H and of the redundant and synergistic contributions, while this does not occur for mental stress given the different trends between unique and redundant contributions and the invariance of synergy.

The comparison between model-free and model-based estimates of the decomposition of the CV PI based on PID (Fig. 3 vs. Fig. 4) highlights an increased predictability of HP during postural stress consistently detected by both approaches, which originates from all PID terms except the unique contribution of SAP. Only the model-free method detects increased CV PI during mental stress, which is due to an increase of the unique contribution of HP and is masked by a concomitant decrease of redundancy when using the model-based method.

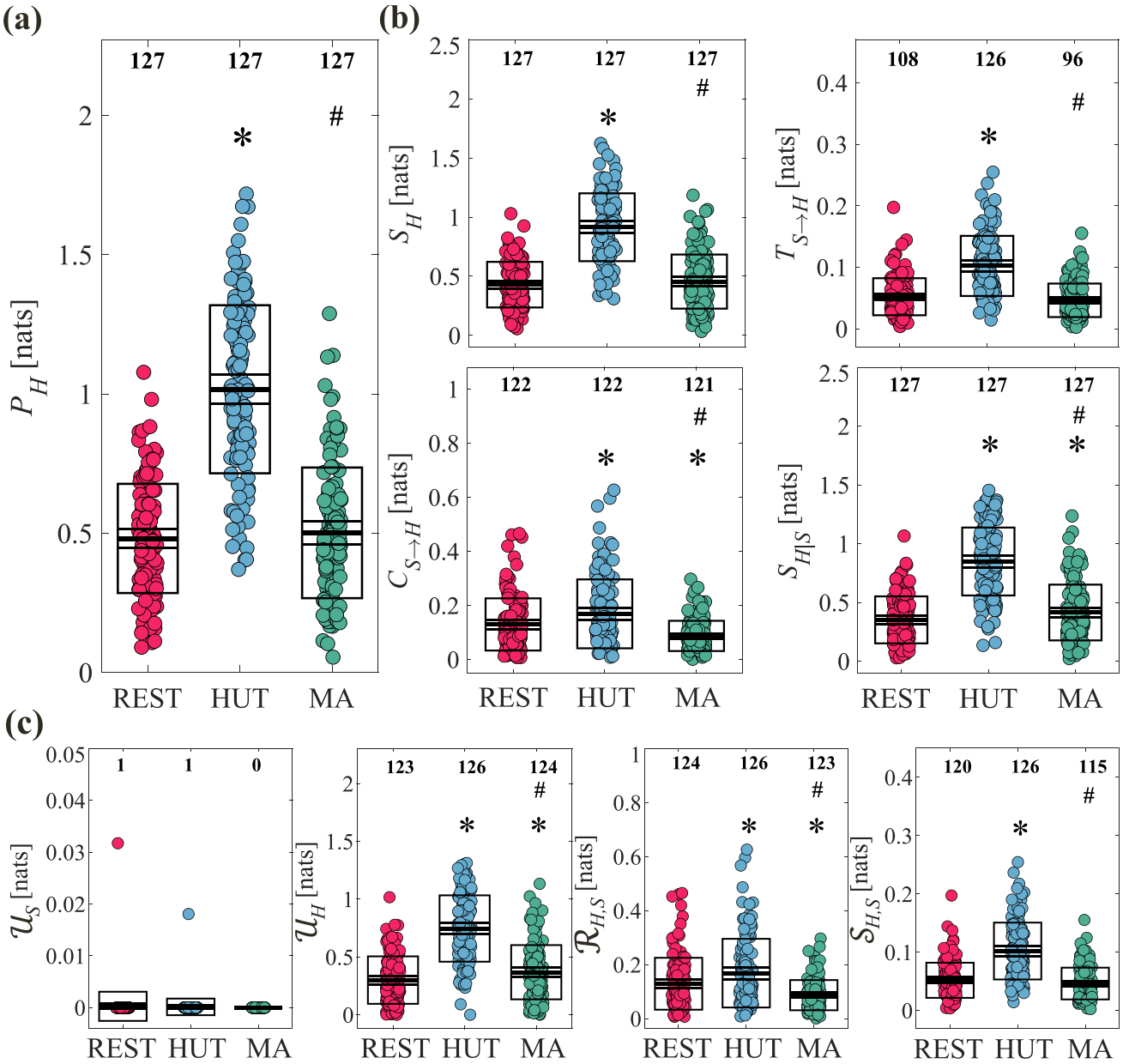

Fig. 4 Predictive Information decomposition of CV interactions obtained via model-based estimates of information dynamics. Plots depict the boxplot distributions and individual values (dots along the vertical lines) of **a** the Predictive Information of H (P_H), **b** the individual terms of the first and second decomposition of P_H given S, and **c** the unique, redundant and synergistic atoms of PID decomposing P_H given S. Measures were evaluated in the REST (red), HUT (blue), and MA (green) conditions. In all panels, black horizontal lines indicate mean values, while the white areas bounded by the box edges and by the lines surrounding the mean represent one standard deviation and the 95% confidence interval, respectively. One-way ANOVA test among conditions ($p < 0.05$): #. Student t-test for paired data with Bonferroni correction for multiple comparison ($p < 0.025$): *REST vs. HUT, REST vs. MA. Values above each distribution indicate the number of subjects (out of 127) for which the measure was deemed as statistically significant according to surrogate data analysis

4.2 Predictive Information decomposition of cardiorespiratory dynamics

Figures 5 and 6 display the results of model-free and model-based dynamic information measures analyses for the assessment of CR interactions evaluated for each subject across the three experimental conditions. Both approaches showed a statistically significant increase of P_H, S_H and $S_{H|R}$, and a significant decrease of $T_{R\to H}$ and $C_{R\to H}$ moving from rest to postural stress (Figs. 5a, b, 6a, b). Applying PID, the increase of P_H is ascribed entirely to a strong increase of $\mathcal{U}_H$ moving from REST to HUT, only partially compensated by a decrease of $\mathcal{U}_R$ and by decreases of $\mathcal{S}_{H,R}$ (seen only with the model-free method) and of $\mathcal{R}_{H,R}$ (seen only with the model-based method) (Figs. 5c, 6c). As regards the response to mental stress, a decrease of P_H was observed moving from REST to MA (significant only using the model-free approach, (Fig. 5a). Using the traditional PI decomposition, such a decrease is ascribed to a decrease of $T_{R\to H}$ and $C_{R\to H}$, only partially compensated by an increase of S_H (using the model-free estimator, Fig. 5b) and of $S_{H|R}$ (using the model-based estimator, Fig. 6b). Using the PID decomposition of the PI, the decrease during MA (seen only with the model-free approach) is ascribed to a decrease of the unique contribution of R, redundancy and synergy ($\mathcal{U}_R$, $\mathcal{R}_{H,R}$, $\mathcal{S}_{H,R}$), only partially compensated by an increase of the unique contribution of H ($\mathcal{U}_H$) (Fig. 5c).

These results suggest that: (i) postural stress and mental stress elicit respectively an increase and a decrease of the predictability of HP variability given its past and the past of RESP; (ii) using the traditional PI decomposition these changes in the PI are ascribed to an increase of the measures reflecting the self-dynamics of HP (SE and cSE) during postural stress and to a decrease of the measures reflecting dynamic coupling (TE and CE) during mental stress; (iii) the PID of the PI reveals that the higher self-predictability during postural stress is driven by stronger unique effects of the past of HP on its present, while the lower cross-predictability during mental stress is driven by weaker redundancy between the past of HP and RESP in determining the present HP.

The comparison between model-free and model-based estimates of the CR PI based on PID (Fig. 5 vs. Fig. 6) highlight a general agreement between the two approaches, with the only exception of a significantly better capability of the model-free approach to detect unique contributions of respiration to the HP dynamics in both stressor conditions.

4.3 Synergy vs. Redundancy in cardiovascular and cardiorespiratory dynamics

Figure 7 depicts the results of the computation of the redundancy/synergy balance measured by taking the difference between redundant an synergistic information, $\Delta_{\mathcal{R}-\mathcal{S}} = \mathcal{R}(Y_n; Y_n^-, X_n^-) - \mathcal{S}(Y_n; Y_n^-, X_n^-)$, computed for each subject using both model-based and model-free methods considering CV interactions (Fig. 7a) and CR interactions (Fig. 7b). The results document that there is a general tendency to net synergy (negative values of $\Delta_{\mathcal{R}-\mathcal{S}}$), as the synergy was found to be prevalent over redundancy in both CV and CR interactions when computed using the model-free estimator, and for CR interactions using the model-based estimator; on the other hand, redundancy was significantly higher than synergy when assessed for CV interactions using the model-based estimator.

The detected prevalence of synergy observed when using the model-free approach to PID indicates that HP variability is predicted through a non-trivial interaction between the HP dynamics and the dynamics of SAP or RESP. Moreover, given the generally small unique contribution of the past of SAP or the past of RESP to the present of HP (Figs. 3, 4, 5, 6), the synergistic interaction seems the main factor sustaining the causal effects from SAP to HP and from RESP to HP measured by the transfer entropies $T_{S\to H}$ and $T_{R\to H}$ in the various experimental conditions.

5 Discussion

5.1 Partial decomposition of heart period predictive information

The present work introduced an approach to decompose the information carried over time by bivariate dynamic systems into amounts related to the dynamics of the individual system components and amounts related to the interaction between such components. The proposed decomposition exploits PID to refine a previously proposed approach [22] whereby the PI, measured as the information shared between the present state of an individual target system and the past states of the joint bivariate system, is decomposed using standard information theory via the chain rule for the MI. The improvement led by the new method stands in the ability to explicitly separate the unique contributions to the analyzed PI attributable to the internal dynamics of the target system from the contributions shared between the target and the driver systems, also distinguishing redundant and synergistic parts in the latter. Our method is related to the more sophisticated integrated information decomposition [52] recently proposed to dissect the information flowing in bivariate systems; the difference is in the fact that, using

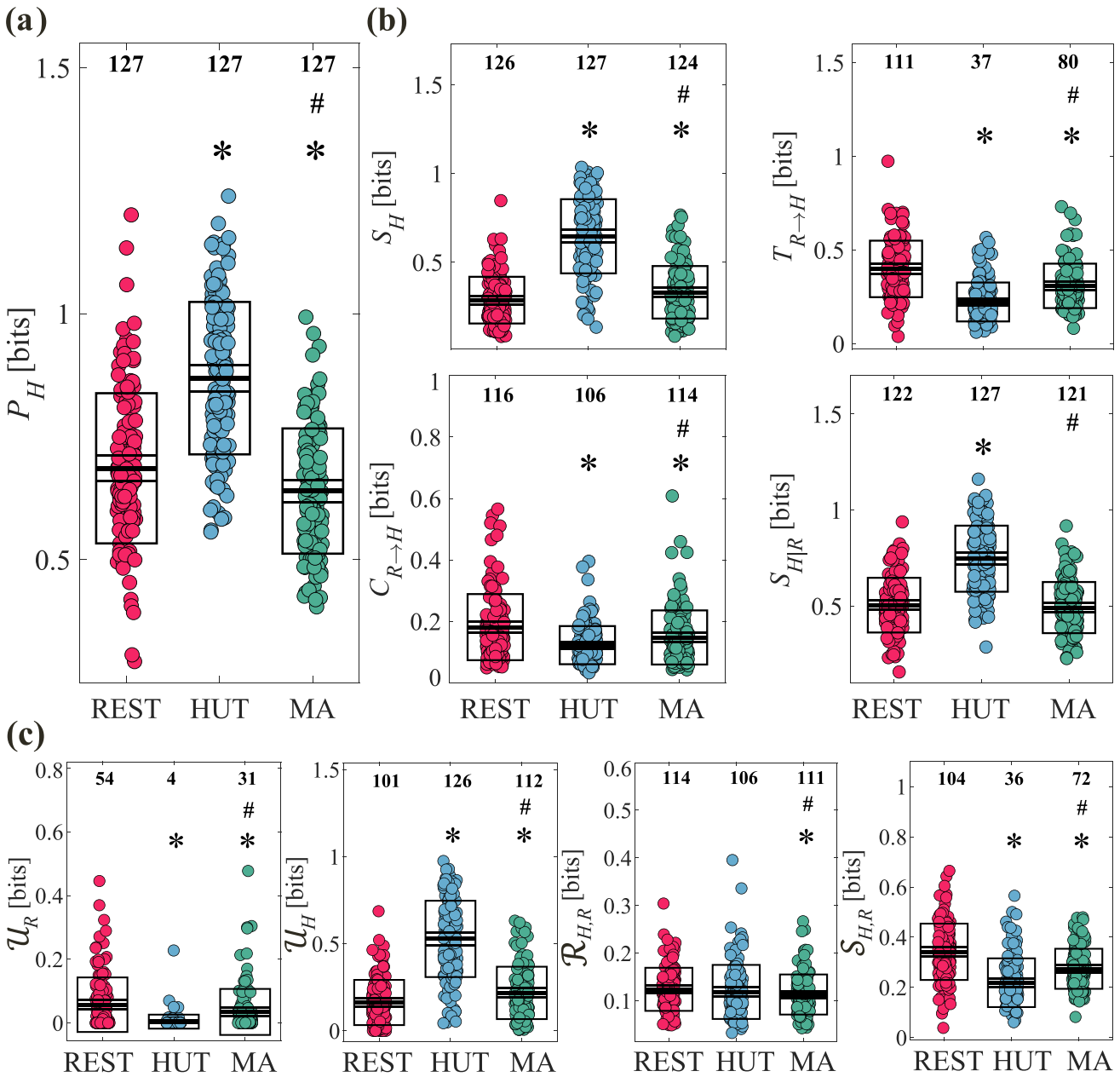

Fig. 5 Predictive Information decomposition of CR interactions obtained via model-free estimates of information dynamics. Plots depict the boxplot distributions and individual values (dots along the vertical lines) of **a** the Predictive Information of H (P_H), **b** the individual terms of the first and second decomposition of P_H given R, and **c** the unique, redundant and synergistic atoms of PID decomposing P_H given R. Measures were evaluated in the REST (red), HUT (blue), and MA (green) conditions. In all panels, black horizontal lines indicate mean values, while the white areas bounded by the box edges and by the lines surrounding the mean represent one standard deviation and the 95% confidence interval, respectively. One-way ANOVA test ($p < 0.05$): $^{\#}$Student t-test for paired data with Bonferroni correction for multiple comparison ($p < 0.025$): *REST vs. HUT, REST vs. MA. Values above each distribution indicate the number of subjects (out of 127) for which the measure was deemed as statistically significant according to surrogate data analysis

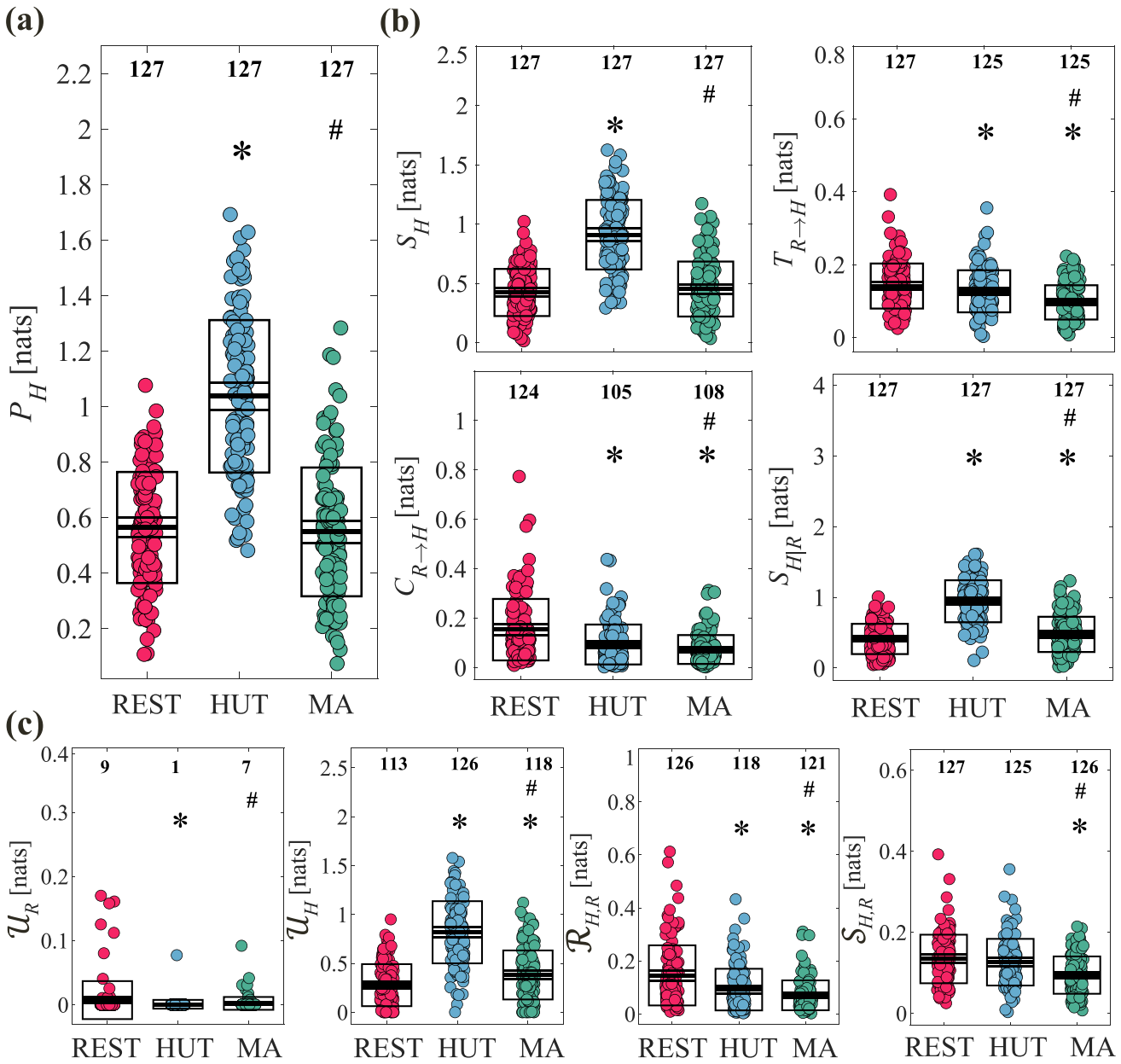

Fig. 6 Predictive Information decomposition of CR interactions obtained via model-based estimates of information dynamics. Plots depict the boxplot distributions and individual values (dots along the vertical lines) of **a** the Predictive Information of H (P_H), **b** the individual terms of the first and second decomposition of P_H given R, and **c** the unique, redundant and synergistic atoms of PID decomposing P_H given R. Measures were evaluated in the REST (red), HUT (blue), and MA (green) conditions. In all panels, black horizontal lines indicate mean values, while the white areas bounded by the box edges and by the lines surrounding the mean represent one standard deviation and the 95% confidence interval, respectively. One-way ANOVA test among conditions ($p < 0.05$): $^{\#}$Student t-test for paired data with Bonferroni correction for multiple comparison ($p < 0.025$): *REST vs. HUT, REST vs. MA. Values above each distribution indicate the number of subjects (out of 127) for which the measure was deemed as statistically significant according to surrogate data analysis

a single target and two sources, our approach can be implemented through the standard redundancy lattice used for the PID rather than the double redundancy lattice needed when also the target is multivariate.

The possibility offered by the proposed decomposition to separate unique and shared contributions within the PI, and redundant and synergistic contributions within the shared information, allowed us to disentangle in a more refined way the statistical relationships underlying the joint CV and CR dynamics studied when HP is the target of the PI, and SAP or RESP is the driver. Specifically, we found that: (i) the unique information provided to the present HP by its own past values is always significant and larger than the unique contribution provided

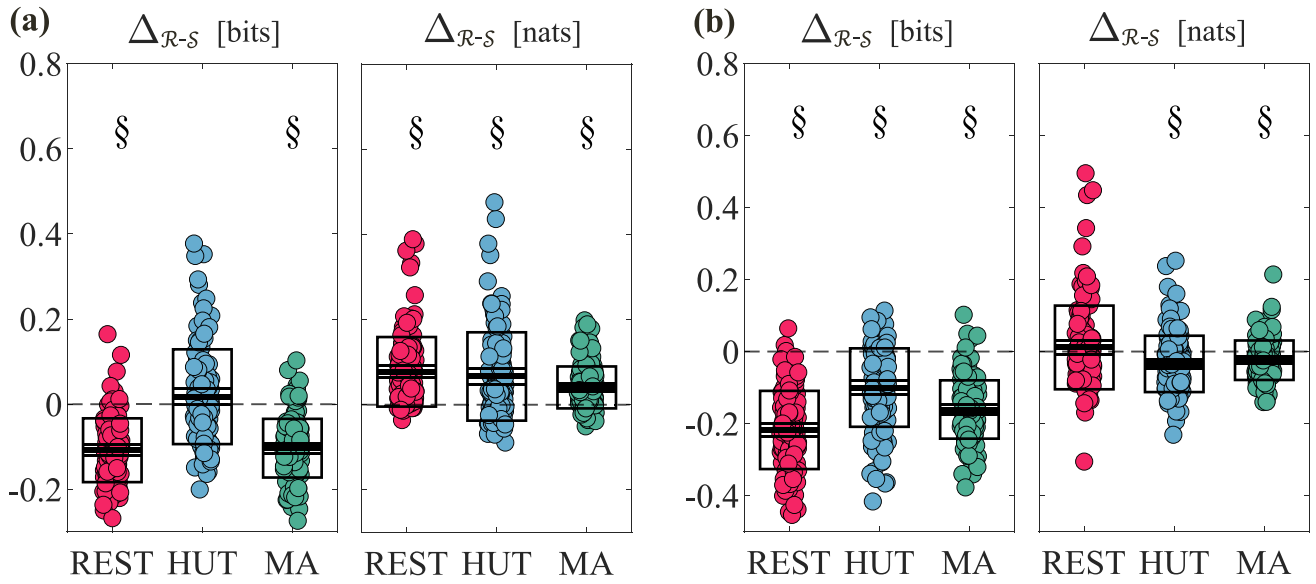

Fig. 7 Plots depict the boxplot distributions and the individual values (dots along the vertical lines) of the redundant-synergy balance ($\Delta_{\mathcal{R}-\mathcal{S}} = \mathcal{R} - \mathcal{S}$) computed for CV (**a**) and CR (**b**) dynamics in both model-free (left subpanel, in bits) and model-based (right subpanel, in nats) formulations. Measures were evaluated in the REST (red), HUT (blue), and MA (green) conditions. In all panels, black horizontal lines indicate mean values, while the white areas bounded by the box edges and by the lines surrounding the mean represent one standard deviation and the 95% confidence interval, respectively. Student t-test for paired data ($p < 0.05$): §, $\mathcal{R}$ vs. $\mathcal{S}$

by the past of SAP or RESP, which on the contrary is very small or negligible; (ii) the unique information of HP given its past drives the significant increase of the dynamic information measures reflecting the regularity of heart rate variability (i.e., SE and cSE) observed during physiological stress (especially postural, but also mental); (iii) the changes of the dynamic information measures reflecting CV and CR coupling (i.e., CE and TE) observed in conditions of head-up tilt or mental workload are determined predominantly by the atoms of shared information (redundant and/or synergistic), and only to a negligible extent by the unique information provided by the driver process (either SAP or RESP).

These results suggest that the proposed framework is important for the investigation of the neural physiological mechanisms that determine the short-term heart rate variability accounting for self-loops as well as CV and CR interactions [53]. According to seminal works in Physiology [54–58] these mechanisms may include feedback circuits producing oscillations at the frequency of the arterial pressure Mayer waves (around 0.1 Hz) due to resonance properties or to the delay inherent to circuit (e.g., baroreflex, chemoreflex), native self-sustained oscillators (e.g., vasomotor and respiratory centers, peripheral vasomotion), and effects of respiration on heart rate, both directed to the sinus node or mediated by arterial pressure. These mechanisms have been related to the PI of short-term HP variability [23] and to its components obtained from the standard decomposition based on MI [59]. In the next subsections we reinterpret these findings about CV and CR dynamics in the light of our more refined decomposition based on PID.

5.2 Assessment of cardiovascular dynamics via predictive information decomposition

The existence of evident CV interactions was documented by the high and statistically significant amount of information conveyed from the past states of HP and SAP to the current HP value, detected in all subjects and experimental conditions (Figs. 2, 3). The PI increased significantly with postural stress, as a result of an increase of the measures reflecting both the regularity of HP and the coupling with SAP. On the contrary, the PI did not change substantially with mental stress, reflecting a balance between mild tendencies to higher regularity of HP and lower coupling between HP and SAP. These results are obtained by analyzing the trends of the measures of regularity (SE, cSE) and directed coupling (CE, TE) obtained from the MI-based decomposition of the PI, and confirm previous finding in the literature [8, 23, 26, 27, 30, 59–61]. Specifically, it is well-known that the shift in the sympatho-vagal balance toward sympathetic activation and parasympathetic deactivation induced by postural stress is reflected by a higher regularity of the HP dynamics [26, 27, 62] and a higher causal coupling between SAP and HP [8, 23, 63]. Previous studies have also documented that the regularity of HP and the coupling from

SAP to HP are barely affected by mental workload [59, 64], indicating a less evident neuroautonomic modulation in this case.

The utilization of PID allowed us to refine the above results identifying the information atoms which are related to stress-induced variations of information dynamics. The first important finding was that the increased regularity of HP observed evidently during head-up tilt and mildly during mental workload is due to the unique information of the HP process, while the shared information (synergistic or redundant) may mask the variations of SE and cSE especially during mental workload (Figs. 2, 3). This indicates the unique information of HP as a better marker than information storage of the sympathetic activation induced by postural and mental stress. Moreover, PID highlights that the tilt-induced increase in CV coupling documented by the higher CE and TE from SAP to HP is driven by an increase of both the redundant and the synergistic shared information; also the reduced CE detected during MA by the model-based method is associated with a concomitant decrease of the redundant information. This suggests that the shared information of SAP and HP, more than the unique information of SAP, is crucial to sustain the SAP-HP directed coupling and its changes related to stress.

Physiologically, these results could be linked to previously hypothesized mechanisms of generation of slow, regular oscillations in HP variability, i.e. the presence of low-frequency oscillations at a central level in the brainstem which are transmitted to the sinus node [56], or to a resonance of short-term regulation of arterial pressure sustained by closed-loop interaction between SAP and HP [55]. Specifically, independent mechanisms of central origin are compatible with the presence of unique information within HP, while vascular resonance could be supported by redundant and especially synergistic information shared between SAP and HP. These associations would suggest that both mechanisms are present in resting humans, and are enhanced by physiological stress.

5.3 Assessment of cardiorespiratory dynamics via predictive information decomposition

The analysis of joint CR dynamics documented that the PI of HP given its past and the past of RESP was always statistically significant and displayed an evident increase during head-up tilt as well as a tendency to decrease during mental workload (Figs. 5, 6). These trends resulted from an increase of the measures reflecting the regularity of HP (SE, cSE) induced by tilt and of a decrease of the measures reflecting the coupling with RESP (CE, TE) induced by the mental arithmetic task. Similar alterations of information measures reflecting the regularity of HP dynamics during orthostatic stress and cardiorespiratory interactions during both orthostatic stress and cognitive load were observed in previous studies [59], and related to the known decrease of parasympathetic activity mainly observed with these types of physiological stress [13, 65].

The decomposition of CR information dynamics performed by PID confirmed the impact that the unique contribution of the past of HP to its present has on the increased regularity during postural stress, and indicated the shared information (both redundant and synergistic) as the determinant of the lower coupling directed from RESP to HP observed during mental stress. These results are in line with those obtained in the analysis of CV interactions as regards the main roles played by the unique and shared information in driving measures of regularity and coupling, respectively. Physiologically, the unique information of HP assumes the same meaning as in the CV analysis, reflecting self-dependencies within the HP that are independent of respiration and are thus likely related to the low frequency interplay between theMayer waves of arterial pressure and the heart rhythm [53, 55, 56]. On the other hand, CR dynamics results mainly from the effect of the respiratory input on the short-term variability of heart rate, which is exerted over two distinct pathways: the direct effect on the sinus node of the respiratory rhythms generated at a central level [57], and the reflex modulation of the sinus node in response to arterial pressure changes mechanically induced by respiration [58]. The analyzed redundant and synergistic shared information should incorporate effects occurring along both these pathways, since arterial pressure variability is not included in the study of CR dynamics and thus cannot be disentangled. Future work is envisaged to investigate more complex multivariate interactions through a PID with three source variables.

5.4 Methodological considerations

The present work integrates PID within the decomposition of the predictive information of a bivariate dynamic system. It is important to acknowledge that the PID framework is not univocal as regards the definition of redundancy that needs to be provided to solve the PID equations. In the rich literature about PID, several works have proposed alternative measures of redundancy, which are grounded in a multitude of different and partly non-compatible desiderata [35, 66]; as a consequence, quantitative results may depend on the formulation adopted. In this work, the proposed approach to decompose the PI of cardiovascular time series was implemented according to two redundancy definitions, which entail also the use of different estimation approaches: the model-free computation of the specific MI redundancy [34], and the model-based computation of the minimum MI redundancy [36]. When implemented on short realizations like in this case according to the typical setting of cardiovascular variability studies featuring time series of 300 heartbeats, the two strategies deal with computational issues (mainly, the curse of dimensionality) in a different way [67]: the model-based approach can afford longer memories since it

relies on the compact model structure where only few parameters need to be estimated from data, at the price of losing the capability to detect strongly nonlinear behaviors; the model-free approach discretizes the amplitude of the time series samples and limits the memory to an extent that is compatible with the estimation of probability distributions in multi-dimensional spaces.

The fact that the two approaches provide in most cases consistent outcomes, with similar changes detected in both standard (MI-based) and novel (PID-based) measures, highlights that nonlinearities may play a negligible role for the specific application and dataset taken into account. This documents the robustness of the obtained findings at varying the definition of redundancy adopted, the estimation strategy and the parameter setting. One notable exception is the detection of a certain number (up to more than 40% of subjects) of statistically significant values of the unique information from RESP to HP detected only by the model-free approach. This may be indicative of the appropriateness of the redundancy measure based on the specific MI, as the minimum MI typically overestimates redundancy at the price of smaller unique contributions [68], and of the presence of nonlinearities of respiratory effects, which have been previously hypothesized [69, 70] and here could not be detected by the linear model-based method.

Another methodological remark regards the model order selection in the model-based approach, performed in this work using the AIC criterion while scanning a relatively high number of delays (up to 12). This approach should ensure that the model captures all the time-lagged effects that typically occur with different maximum latency within and between HP and SAP due to their different complexity [71].

Finally, it is worth noting that the redundancy–synergy balance, plotted in Fig. 7, reveals a predominance of synergistic over redundant contributions. This result, together with the generally small unique effects, suggests that CV and CR causal interactions typically evidenced by the transfer entropy [22, 72] are sustained mostly by a complex synergistic interplay between the driver (SAP or RESP) and the target HP. The detection of net synergy marks a difference with previous studies on CV and CR interactions, instead reporting redundancy as typically dominant [73]. This different behavior can be attributed to the inclusion, in our framework, of the target's own past as one of the sources, which appears to enhance synergistic interactions among the considered processes. Therefore, our results derived from the PID analysis of bivariate time series do not contradict the general tendency of cardiovascular-respiratory interaction to highlight prevalent redundancy over synergy shown by methods working on triplets of time series [73, 74]. Moreover, it is worth emphasizing that the concept of synergy quantified by PID and information-theoretic measures applied to time series data reflects a structure of statistical dependence among random variables, which does not necessarily imply the existence of direct mechanistic synergy in the rules governing the causal evolution of the analyzed system. The distinction between these two complementary concepts of synergy is at the core of the comparison between high-order mechanisms and high-order behaviors [75], and constitutes an active area of research also in the context of cardiovascular variability analysis [76].

6 Conclusion

This work introduced a novel application of the PID framework to information decomposition in dynamic bivariate systems, aimed to achieve a better dissection of internal and coupled dependencies than that guaranteed by classical decompositions based on Shannon mutual information. The new formulation evidences that, even if PI and its traditional decomposition terms (i.e., SE, cSE, TE, and CE) often explain well expected behaviors, their conventional interpretation as purely causal indicators, reflecting information uniquely attributable to the target by its past or the driver's past, can be intrinsically ambiguous. When applied to the dynamics of CV and CR control systems probed in young healthy subjects at rest and during orthostatic stress and cognitive load, the new framework highlights that the target HP dynamics are inherently driven by their internal history considered individually or in combination with the history of the putative driver dynamics (either SAP or RESP) producing higher-order interactions.

Overall, the proposed framework bridges a gap in information-theoretic computational physiology by disentangling how information is distributed, co-localized, and jointly generated within interconnected physiological networks. Beyond methodological innovation, the proposed approach offers a new interpretive key for understanding how autonomic control emerges from multiple dynamical sources. Future works should also envisage the spectral decomposition of PID (also using the corresponding measures for random processes [77, 78]) to HP and SAP variability in order to provide further physiological insights. Additionally, since the setting of the latency of interactions plays an important role in CR interactions, as the HP-RESP relation depends on respiratory rate [79], future studies could be designed to test physiologically plausible delays in both the RESP→HP and HP→RESP directions, thus also assessing the role of latencies in closed-loop CR dynamics. Finally, future extensions to multivariate and pathological data may establish the balance among unique, redundant, and synergistic information as a sensitive indicator of altered network coordination and loss of physiological adaptability.

Acknowledgements This work was supported by the projects "HONEST—High-Order Dynamical Networks in Computational Neuroscience and Physiology: an Information-Theoretic Framework", Italian Ministry of University and Research (funded by MUR, PRIN 2022, code 2022YMHNPY, CUP: B53D23003020006) and "DARE—Digital lifelong pRevEntion initiative" (MUR, PNC D.D. 931 06/06/2022, code PNC0000002). R.S. was supported by DARE project.

Author contribution statement

Roberta Saputo: writing—original draft, visualization, validation, software, methodology, formal analysis, data curation, conceptualization. Chiara Barà: writing—original draft, methodology, software, data curation. Irene Franzone: methodology, software, data curation. Michal Javorka: Data curation; writing—review and editing. Riccardo Pernice: writing—review and editing; methodology, investigation, supervision. Luca Faes: writing—review and editing, validation, supervision, software, resources, project administration, methodology, investigation, funding acquisition, conceptualization.

Funding Open access funding provided by Università degli Studi di Palermo within the CRUI-CARE Agreement.

Data availability Data used in the present study are available from the authors on reasonable request.

Declarations

Conflict of interest The authors declare that they have no competing financial interests or personal relationships that could have appeared to influence the work reported in this paper.

References

1. H. Sayama, *Introduction to the Modeling and Analysis of Complex Systems* (Open SUNY Textbooks, New York, 2015)
2. A. Bashan, R.P. Bartsch, J.W. Kantelhardt, S. Havlin, P.C. Ivanov, Network physiology reveals relations between network topology and physiological function. Nat. Commun. **3**(1), 702 (2012)
3. P.C. Ivanov, The new field of network physiology: building the human physiolome. Front. Netw. Physiol. **1**, 711778 (2021)
4. M. Elstad, E.L. O'Callaghan, A.J. Smith, A. Ben-Tal, R. Ramchandra, Cardiorespiratory interactions in humans and animals: rhythms for life. Am. J. Physiol. Heart Circ. Physiol. **315**(1), H6–H17 (2018)
5. G. Parati, P. Castiglioni, A. Faini, M. Di Rienzo, G. Mancia, R. Barbieri, J.P. Saul, Closed-loop cardiovascular interactions and the baroreflex cardiac arm: modulations over the 24 h and the effect of hypertension. Front. Physiol. **10**, 477 (2019)
6. P.A. Lanfranchi, V.K. Somers, Arterial baroreflex function and cardiovascular variability: interactions and implications. Am. J. Physiol. Regul. Integr. Comp. Physiol. **283**(4), R815–R826 (2002)
7. S. Charleston-Villalobos, S. Reulecke, A. Voss, M.R. Azimi-Sadjadi, R. González-Camarena, M.J. Gaitán-González, J.A. González-Hermosillo, G. Hernández-Pacheco, S. Schulz, T. Aljama-Corrales, Time-frequency analysis of cardiovascular and cardiorespiratory interactions during orthostatic stress by extended partial directed coherence. Entropy **21**(5), 468 (2019)
8. L. Faes, G. Nollo, A. Porta, Mechanisms of causal interaction between short-term rr interval and systolic arterial pressure oscillations during orthostatic challenge. J. Appl. Physiol. **114**(12), 1657–1667 (2013)
9. M. Javorka, J. Krohova, B. Czippelova, Z. Turianikova, Z. Lazarova, K. Javorka, L. Faes, Basic cardiovascular variability signals: mutual directed interactions explored in the information domain. Physiol. Meas. **38**(5), 877 (2017)
10. M. Zanetti, L. Faes, G. Nollo, M. De Cecco, R. Pernice, L. Maule, M. Pertile, A. Fornaser, Information dynamics of the brain, cardiovascular and respiratory network during different levels of mental stress. Entropy **21**(3), 275 (2019)
11. L. Bernardi, C. Porta, L. Spicuzza, P. Sleight, Cardiorespiratory interactions to external stimuli. Arch. Ital. Biol. **143**(3–4), 215–221 (2005)
12. D. Widjaja, M. Orini, E. Vlemincx, S. Van Huffel, Cardiorespiratory dynamic response to mental stress: a multivariate time-frequency analysis. Comput. Math. Methods Med. **2013**(1), 451857 (2013)
13. W.H. Cooke, J.B. Hoag, A.A. Crossman, T.A. Kuusela, K.U. Tahvanainen, D.L. Eckberg, Human responses to upright tilt: a window on central autonomic integration. J. Physiol. **517**(2), 617–628 (1999)

14. L. Faes, G. Nollo, Bivariate nonlinear prediction to quantify the strength of complex dynamical interactions in short-term cardiovascular variability. Med. Biol. Eng. Comput. **44**(5), 383–392 (2006)
15. M. Baumert, M. Javorka, M. Kabir, Joint symbolic dynamics for the assessment of cardiovascular and cardiorespiratory interactions. Philos. Trans. R. Soc. A Math. Phys. Eng. Sci. **373**(2034), 20140097 (2015)
16. R.M.D. Abreu, B. Cairo, A. Porta, On the significance of estimating cardiorespiratory coupling strength in sports medicine. Front. Netw. Physiol. **2**, 1114733 (2023)
17. M.M. Platiša, N.N. Radovanović, R. Pernice, C. Barà, S.U. Pavlović, L. Faes, Information-theoretic analysis of cardiorespiratory interactions in heart failure patients: effects of arrhythmias and cardiac resynchronization therapy. Entropy **25**(7), 1072 (2023)
18. J.T. Lizier, *The Local Information Dynamics of Distributed Computation in Complex Systems* (Springer Science & Business Media, Cham, 2012)
19. W. Bialek, I. Nemenman, N. Tishby, Predictability, complexity, and learning. Neural Comput. **13**(11), 2409–2463 (2001)
20. L. Faes, G. Mijatovic, L. Sparacino, A. Porta, Predictive information decomposition as a tool to quantify emergent dynamical behaviors in physiological networks. IEEE Trans. Biomed. Eng. **72**(12), 3515–3524 (2025)
21. M. Wibral, R. Vicente, J.T. Lizier, *Directed Information Measures in Neuroscience*, vol. 724 (Springer, Berlin, 2014)
22. L. Faes, A. Porta, G. Nollo, Information decomposition in bivariate systems: theory and application to cardiorespiratory dynamics. Entropy **17**(1), 277–303 (2015)
23. L. Faes, D. Kugiumtzis, G. Nollo, F. Jurysta, D. Marinazzo, Estimating the decomposition of predictive information in multivariate systems. Phys. Rev. E **91**(3), 032904 (2015)
24. M. Wibral, J.T. Lizier, S. Vögler, V. Priesemann, R. Galuske, Local active information storage as a tool to understand distributed neural information processing. Front. Neuroinform. **8**, 1 (2014)
25. T. Schreiber, Measuring information transfer. Phys. Rev. Lett. **85**(2), 461 (2000)
26. L. Faes, A. Porta, G. Rossato, A. Adami, D. Tonon, A. Corica, G. Nollo, Investigating the mechanisms of cardiovascular and cerebrovascular regulation in orthostatic syncope through an information decomposition strategy. Auton. Neurosci. **178**(1–2), 76–82 (2013)
27. L. Faes, M.A. Pereira, M.E. Silva, R. Pernice, A. Busacca, M. Javorka, A.P. Rocha, Multiscale information storage of linear long-range correlated stochastic processes. Phys. Rev. E **99**(3), 032115 (2019)
28. I. Lazic, R. Pernice, T. Loncar-Turukalo, G. Mijatovic, L. Faes, Assessment of cardiorespiratory interactions during apneic events in sleep via fuzzy kernel measures of information dynamics. Entropy **23**(6), 698 (2021)
29. D. Makowiec, A. Kaczkowska, D. Wejer, M. Żarczyńska-Buchowiecka, Z.R. Struzik, Entropic measures of complexity of short-term dynamics of nocturnal heartbeats in an aging population. Entropy **17**(3), 1253–1272 (2015)
30. D. Wejer, L. Faes, D. Makowiec, Causal relationships in the variability of cardiovascular system evoked by orthostatic stress by transfer entropy, in *2015 37th Annual International Conference of the IEEE Engineering in Medicine and Biology Society (EMBC)* (IEEE, 2015), pp. 3799–3802
31. D. Wejer, B. Graff, D. Makowiec, S. Budrejko, Z.R. Struzik, Complexity of cardiovascular rhythms during head-up tilt test by entropy of patterns. Physiol. Meas. **38**(5), 819 (2017)
32. D. Makowiec, D. Wejer, B. Graff, Z.R. Struzik, Dynamical pattern representation of cardiovascular couplings evoked by head-up tilt test. Entropy **20**(4), 235 (2018)
33. R.G. James, N. Barnett, J.P. Crutchfield, Information flows? A critique of transfer entropies. Phys. Rev. Lett. **116**(23), 238701 (2016)
34. P.L. Williams, R.D. Beer, Nonnegative decomposition of multivariate information (2010). arXiv preprint arXiv:1004.2515
35. J.T. Lizier, N. Bertschinger, J. Jost, M. Wibral, Information decomposition of target effects from multi-source interactions: perspectives on previous, current and future work. Entropy **20**(4), 307 (2018)
36. A.B. Barrett, Exploration of synergistic and redundant information sharing in static and dynamical gaussian systems. Phys. Rev. E **91**(5), 052802 (2015)
37. A. Porta, V. Bari, F. Gelpi, B. Cairo, B. De Maria, D. Tonon, G. Rossato, L. Faes, On the different abilities of cross-sample entropy and k-nearest-neighbor cross-unpredictability in assessing dynamic cardiorespiratory and cerebrovascular interactions. Entropy **25**(4), 599 (2023)
38. A.B. Barrett, L. Barnett, A.K. Seth, Multivariate granger causality and generalized variance. Phys. Rev. E Stat. Nonlinear Soft Matter Phys. **81**(4), 041907 (2010)
39. H. Lütkepohl, *Introduction to Multiple Time Series Analysis* (Springer Science & Business Media, Cham, 2013)
40. L. Sparacino, Y. Antonacci, C. Barà, A. Valenti, A. Porta, L. Faes, A method to assess granger causality, isolation and autonomy in the time and frequency domains: theory and application to cerebrovascular variability. IEEE Trans. Biomed. Eng. **71**(5), 1454–1465 (2023)
41. G. Mijatovic, Y. Antonacci, M. Javorka, D. Marinazzo, S. Stramaglia, L. Faes, Network representation of higher-order interactions based on information dynamics. IEEE Trans. Netw. Sci. Eng. **12**(3), 1872–1884 (2025)
42. M. Iovino, I. Lazic, T. Loncar-Turukalo, M. Javorka, R. Pernice, L. Faes, Comparison of automatic and physiologically-based feature selection methods for classifying physiological stress using heart rate and pulse rate variability indices. Physiol. Meas. **45**(11), 115004 (2024)
43. R. Pernice, M. Javorka, J. Krohova, B. Czippelova, Z. Turianikova, A. Busacca, L. Faes, Comparison of short-term heart rate variability indexes evaluated through electrocardiographic and continuous blood pressure monitoring. Med. Biol. Eng. Comput. **57**(6), 1247–1263 (2019)

44. R. Saputo, M. Iovino, R. Pernice, M. Javorka, L. Faes, Multi-feature classification of physiological stress in cardiovascular and cardiorespiratory interactions, in *2024 13th Conference of the European Study Group on Cardiovascular Oscillations (ESGCO)* (IEEE, 2024), pp. 1–2
45. M. Javorka, F. El-Hamad, B. Czippelova, Z. Turianikova, J. Krohova, Z. Lazarova, M. Baumert, Role of respiration in the cardiovascular response to orthostatic and mental stress. Am. J. Physiol. Regul. Integr. Comp. Physiol. **314**(6), R761–R769 (2018)
46. G. Nollo, L. Faes, B. Pellegrini, A. Porta, R. Antolini, Synchronization index for quantifying nonlinear causal coupling between rr interval and systolic arterial pressure after myocardial infarction, in *Computers in Cardiology 2000 (Cat. 00CH37163)*, vol. 27 (IEEE, 2000), pp. 143–146
47. L. Faes, A. Porta, Conditional entropy-based evaluation of information dynamics physiological systems, in *Directed information measures in neuroscience*. ed. by M. Wibral, R. Vicente, J. Lizier (Springer, 2014), pp. 61–86
48. J. Runge, J. Heitzig, V. Petoukhov, J. Kurths, Escaping the curse of dimensionality in estimating multivariate transfer entropy. Phys. Rev. Lett. **108**(25), 258701 (2012)
49. H. Akaike, A new look at the statistical model identification. IEEE Trans. Autom. Control **19**(6), 716–723 (2003)
50. C. Barà, Y. Antonacci, M. Iovino, I. Lazic, L. Faes, Partial information decomposition for mixed discrete and continuous random variables (2024). arXiv preprint arXiv:2409.13506
51. H. Pinto, I. Lazic, Y. Antonacci, R. Pernice, D. Gu, C. Barà, L. Faes, A.P. Rocha, Testing dynamic correlations and nonlinearity in bivariate time series through information measures and surrogate data analysis. Front. Netw. Physiol. **4**, 1385421 (2024)
52. P.A. Mediano, F.E. Rosas, A.I. Luppi, R.L. Carhart-Harris, D. Bor, A.K. Seth, A.B. Barrett, Toward a unified taxonomy of information dynamics via integrated information decomposition. Proc. Natl. Acad. Sci. **122**(39), e2423297122 (2025)
53. G. Baselli, S. Cerutti, F. Badilini, L. Biancardi, A. Porta, M. Pagani, F. Lombardi, O. Rimoldi, R. Furlan, A. Malliani, Model for the assessment of heart period and arterial pressure variability interactions and of respiration influences. Med. Biol. Eng. Comput. **32**(2), 143–152 (1994)
54. G. Preiss, C. Polosa, Patterns of sympathetic neuron activity associated with Mayer waves. Am. J. Physiol. Leg. Content **226**(3), 724–730 (1974)
55. R.W. DeBoer, J.M. Karemaker, J. Strackee, Hemodynamic fluctuations and baroreflex sensitivity in humans: a beat-to-beat model. Am. J. Physiol. Heart Circ. Physiol. **253**(3), H680–H689 (1987)
56. H. Koepchen, Physiology of rhythms and control systems: an integrative approach, in *Rhythms in Physiological Systems: Proceedings of the International Symposium at Schloß Elmau, Bavaria, October 22–25, 1990* (Springer, 1991), pp. 3–20
57. D.L. Eckberg, Point: counterpoint: respiratory sinus arrhythmia is due to a central mechanism vs. respiratory sinus arrhythmia is due to the baroreflex mechanism. J. Appl. Physiol. **106**(5), 1740–1744 (2009)
58. J.M. Karemaker, Counterpoint: respiratory sinus arrhythmia is due to the baroreflex mechanism. J. Appl. Physiol. **106**(5), 1742–1743 (2009)
59. M. Javorka, J. Krohova, B. Czippelova, Z. Turianikova, Z. Lazarova, R. Wiszt, L. Faes, Towards understanding the complexity of cardiovascular oscillations: insights from information theory. Comput. Biol. Med. **98**, 48–57 (2018)
60. L. Faes, G. Nollo, A. Porta, Non-uniform multivariate embedding to assess the information transfer in cardiovascular and cardiorespiratory variability series. Comput. Biol. Med. **42**(3), 290–297 (2012)
61. A. Porta, L. Faes, G. Nollo, V. Bari, A. Marchi, B. De Maria, A.C. Takahashi, A.M. Catai, Conditional self-entropy and conditional joint transfer entropy in heart period variability during graded postural challenge. PLoS ONE **10**(7), e0132851 (2015)
62. L. Faes, D. Marinazzo, S. Stramaglia, Multiscale information decomposition: exact computation for multivariate gaussian processes. Entropy **19**(8), 408 (2017)
63. A. Porta, A.M. Catai, A.C. Takahashi, V. Magagnin, T. Bassani, E. Tobaldini, P. Van De Borne, N. Montano, Causal relationships between heart period and systolic arterial pressure during graded head-up tilt. Am. J. Physiol. Regul. Integr. Comp. Physiol. **300**(2), R378–R386 (2011)
64. L. Faes, M. Javorka, G. Nollo, Information-theoretic assessment of cardiovascular variability during postural and mental stress, in *XIV Mediterranean Conference on Medical and Biological Engineering and Computing 2016: MEDICON 2016, March 31st–April 2nd 2016, Paphos, Cyprus* (Springer, 2016), pp. 67–70
65. M. Pagani, G. Mazzuero, A. Ferrari, D. Liberati, S. Cerutti, D. Vaitl, L. Tavazzi, A. Malliani, Sympathovagal interaction during mental stress. A study using spectral analysis of heart rate variability in healthy control subjects and patients with a prior myocardial infarction. Circulation **83**(4 Suppl), II43–II51 (1991)
66. A.J. Gutknecht, M. Wibral, A. Makkeh, Bits and pieces: understanding information decomposition from part-whole relationships and formal logic. Proc. R. Soc. A Math. Phys. Eng. Sci. **477**(2251), 1–28 (2021)
67. C. Barà, R. Pernice, C.A. Catania, M. Hilal, A. Porta, A. Humeau-Heurtier, L. Faes, Comparison of entropy rate measures for the evaluation of time series complexity: simulations and application to heart rate and respiratory variability. Biocybern. Biomed. Eng. **44**(2), 380–392 (2024)
68. F. Rosas, V. Ntranos, C.J. Ellison, S. Pollin, M. Verhelst, Understanding interdependency through complex information sharing. Entropy **18**(2), 38 (2016)
69. J.-O. Fortrat, Y. Yamamoto, R.L. Hughson, Respiratory influences on non-linear dynamics of heart rate variability in humans. Biol. Cybern. **77**(1), 1–10 (1997)
70. M. Sorelli, T.N. Hutson, L. Iasemidis, L. Bocchi, Linear and nonlinear directed connectivity analysis of the cardio-respiratory system in type 1 diabetes. Front. Netw. Physiol. **2**, 840829 (2022)

71. A. Porta, S. Guzzetti, N. Montano, M. Pagani, V. Somers, A. Malliani, G. Baselli, S. Cerutti, Information domain analysis of cardiovascular variability signals: evaluation of regularity, synchronisation and co-ordination. Med. Biol. Eng. Comput. **38**(2), 180–188 (2000)
72. L. Faes, D. Marinazzo, A. Montalto, G. Nollo, Lag-specific transfer entropy as a tool to assess cardiovascular and cardiorespiratory information transfer. IEEE Trans. Biomed. Eng. **61**(10), 2556–2568 (2014)
73. A. Porta, V. Bari, B. De Maria, A.C. Takahashi, S. Guzzetti, R. Colombo, A.M. Catai, F. Raimondi, L. Faes, Quantifying net synergy/redundancy of spontaneous variability regulation via predictability and transfer entropy decomposition frameworks. IEEE Trans. Biomed. Eng. **64**(11), 2628–2638 (2017)
74. A. Porta, R. Maestri, V. Bari, B. De Maria, B. Cairo, E. Vaini, M.T. La Rovere, G.D. Pinna, Paced breathing increases the redundancy of cardiorespiratory control in healthy individuals and chronic heart failure patients. Entropy **20**(12), 949 (2018)
75. F.E. Rosas, P.A. Mediano, A.I. Luppi, T.F. Varley, J.T. Lizier, S. Stramaglia, H.J. Jensen, D. Marinazzo, Disentangling high-order mechanisms and high-order behaviours in complex systems. Nat. Phys. **18**(5), 476–477 (2022)
76. C. Barà, Y. Antonacci, L. Sparacino, H. Pinto, M. Javorka, S. Stramaglia, L. Faes, Investigating high-order behaviors in multivariate cardiovascular interactions via nonlinear prediction and information-theoretic tools (2025). arXiv preprint arXiv:2512.12709
77. L. Faes, L. Sparacino, G. Mijatovic, Y. Antonacci, L. Ricci, D. Marinazzo, S. Stramaglia, Partial information rate decomposition. Phys. Rev. Lett. **135**(18), 187401 (2025)
78. L. Sparacino, G. Mijatovic, Y. Antonacci, L. Ricci, D. Marinazzo, S. Stramaglia, L. Faes, Decomposing multivariate information rates in networks of random processes. Phys. Rev. E **112**(4), 044313 (2025)
79. B. Cairo, V. Bari, F. Gelpi, B. De Maria, A. Porta, Assessing cardiorespiratory interactions via lagged joint symbolic dynamics during spontaneous and controlled breathing. Front. Netw. Physiol. **3**, 1211848 (2023)